Available online at www.sciencedirect.com
SCIENCE DIRECT®
Energy Conversion and Management 47 (2006) 407–426
ENERGY CONVERSION & MANAGEMENT
www.elsevier.com/locate/enconman

# Optimal operation of thermoelectric cooler driven by solar thermoelectric generator

N.M. Khattab *, E.T. El Shenawy

*National Research Centre, Solar Energy Department, El Behouth Street, Dokki, Giza, Cairo, Egypt*

Received 6 June 2004; received in revised form 19 October 2004; accepted 29 April 2005
Available online 12 July 2005

**Abstract**

The possibility of using a solar thermoelectric generator (TEG) to drive a small thermoelectric cooler (TEC) is studied in the present work. The study includes the theory of both the TEG and the TEC, giving special consideration to determination of the number of TEG modules required to power the TEC to achieve the best performance of the TEG–TEC system all year round.

Commercially available thermoelectric modules (TE) are used in the system. The TEG contains 49 thermocouples and the TEC contains 127 thermocouples. A simple arrangement of plane reflectors that are designed to receive maximum solar energy during noon time is used to heat the TEG.

Performance tests are conducted to determine both the physical properties and the performance curves of the available TE modules. Also, empirical relations describing the performance of the TEG and TEC modules have been established. These relations are used to develop a mathematical model simulating the TEG–TEC system to predict its performance all year round under the actual climatic conditions of Cairo, Egypt (30°N latitude).

The model results are used to determine the number of TEG modules required to drive a single TEC module at maximum cooling capacity. The results show that five thermocouples of the TEG can drive one thermocouple of the TEC, which coincides with the previous theory of the TEG–TEC. This means that 10 of the used TEG modules are required to power the used TEC at optimum performance most times of the year.


*Keywords:* Thermoelectric generator; Thermoelectric cooler; Solar heating; Maximum power

* Corresponding author. Tel.: +20 2 7490240; fax: +20 2 3370931.
*E-mail address:* nag_khb@hotmail.com (N.M. Khattab).

0196-8904/$ - see front matter © 2005 Elsevier Ltd. All rights reserved.
doi:10.1016/j.enconman.2005.04.011

**Nomenclature**

| | |
|---|---|
| $A$ | heating plate area, $m^2$ |
| $h_w$ | wind heat transfer coefficient, $W/m^2$ °C |
| $I$ | current, A |
| $k$ | total thermal conductivity of the thermoelectric module, W/° K |
| $N$ | number of glass layers |
| $Q$ | rate of heat, W |
| $R$ | the total electrical resistance of the thermoelectric module, Ω |
| SI | solar intensity, $W/m^2$ |
| $T$ | temperature, K (except Eqs. (20)–(24) where $T$ is in °C) |
| $U_T$ | top loss coefficient, $W/m^2$ K |
| $V$ | wind speed, m/s |

*Greek letters*

| | |
|---|---|
| $\alpha$ | Seebeck coefficient of module, V/°C |
| $\beta$ | angle of inclination of plate |
| $\Delta T$ | temperature difference, °C |
| $\sigma$ | Stefan–Boltzmann constant $= 5.66 \times 10^{-3}$, $W/m^2$ $K^4$ |
| $\varepsilon_g$ | glass emissivity |
| $\varepsilon_P$ | plate emissivity |
| $\tau\alpha$ | glass transmissivity · plate absorptivity |

*Subscripts*

| | |
|---|---|
| amb | ambient |
| c | cooler |
| g | generator |
| H | hot side |
| L | cold side |
| P | plate |

## 1. Introduction

In remote areas, where the electric grid is not available and the sun shines year round, thermoelectric cooling is one of the best candidates for many applications, such as food refrigeration and storage of medicine. Also, military units or remote oil drilling installations might find them very useful. A TEC operates on the Peltier effect in which the passage of a direct current through a junction between two different semiconductors (n-type and p-type) results in cooling of that junction [1]. One p and one n make up a couple. A TE module can contain one to several hundred couples, which are connected electrically in series and thermally in parallel.

Different from all other cooling systems, thermoelectric cooling does not require any compressor, expansion valves, absorbers, condensers or solution pumps. Moreover, it does not require

working fluids or the utilization of any moving parts. It simply uses electrons rather than refrigerants as a heat carrier. Unlike conventional refrigeration systems, TE systems are not fabricated using chlorofluorocarbons that may be harmful to the environment [2], and besides, it can be driven by clean energy such as solar cells [3].

The TEG, like the TEC, consists of n- and p-semiconductors connected electrically in series and thermally in parallel. Unlike the TEC, heat is supplied at one end of the TEG, while the other end is maintained at a lower temperature with a heat sink [4]. As a result of the temperature difference, a current flows through an external load resistance.

A TEG has the advantage that it can operate from a low grade heat source such as waste heat energy [5]. It is also attractive as a means of converting solar energy into electricity [6]. This is especially so if the electrical load is a TEC.

The TEG and TEC could be a highly compatible combination if special consideration is given to determining the correct ratio between the numbers of couples of each. Ioeff [7], who first studied TE modules, found from thermodynamic analysis that this ratio is a function of the parameter called the figure of merit (which is a function of only the TE material) and the temperature difference across the two parts of the modules.

This ratio could be an optimum if the materials of the TE modules have high values of the figures of merit, and the design conditions are based on the maximum values of the parameters characterizing the performance of the TE modules. Based on the maximum COP, maximum cooling capacity and minimum heat sink temperature, the optimum performance of TECs was studied in Refs. [8,9]. The optimum performance of the TEG was studied on the basis of maximum power output or maximum efficiency in Refs. [4,10].

Except for the work of Vella et al. [11], no works were found that studied the optimum performance of the combined solar TEG–TEC system. Vella et al. [11], in their analysis of a TEC powered by a solar TEG, found that to achieve maximum efficiency of the solar generator and maximum coefficient of performance of the cooler, the ratio of the numbers of couples of each could be as low as unity, even for unconcentrated solar radiation. Their practical operation indicated that a ratio of four TEG couples to power a single TEC couple is preferred in this case (their analysis was based on the TEG and TEC having the same heat sink and figures of merit).

In the last two decades, a variety of TEC and TEG modules have become commercially available in different sizes and materials and, hence, different characteristics. The design of a TEG–TEC system for certain applications requires the physical properties and thermal characteristics of such modules to be determined. The manufacturers of thermoelectric modules usually do not provide this kind of data for their customer or the provided data are not accurate due to variations of the manufacturing process.

Therefore, the present work aims to study the possibility of using a solar TEG to drive a small TEC at optimum performance all year round. The theory of both the TEG and TEC is first presented, giving special consideration to determination of the number of TEG modules required to achieve optimum performance of the TEG–TEC system. Then, the physical properties and the performance curves of the commercially available thermoelectric TEC and TEG are measured from module tests.

The basic equations for both TE modules, together with the performance test results, are used to develop a mathematical model to simulate the performance of the solar powered TEG–TEC system. The model results for the generator performance are first validated with the experimental

test results obtained for the generator operation under the actual conditions of the Cairo climate. Then, the performance of the TEG–TEC system is predicted all year round to determine the optimum number of generators for the best TEC performance.

## 2. Theory and analysis

### 2.1. Thermoelectric cooler

The schematic diagram of the TEC is shown in Fig. 1. Two semiconductors p and n are joined to form two junctions. The cold junction is attached to a metal plate or some other type of heat transfer surface. This surface is exposed to the space or substance to be cooled. The hot junction is attached to some type of surface that would allow rejection of heat to atmospheric air or some other heat sink. An external battery provides the circulation of a direct current through the circuit. When a current $I_c$ is passed through the circuit, five thermoelectric effects (Seebeck effect, Joulean effect, conduction effect, Peltier effect and Thomson effect) will occur [1]. Because of the Peltier effect, the cold plate will be cooled to temperature $T_{Lc}$ and the warm plate will be heated to temperature $T_{Hc}$. Under steady state conditions, the theoretical equations for the TEC performance are given by Threlkeld [1] as:

The cooling capacity

$$Q_{Lc} = \alpha_c I_c T_{Lc} - 0.5 I_c^2 R_c - k_c (T_{Hc} - T_{Lc}) \tag{1}$$

The rate of heat rejected

$$Q_{Hc} = \alpha_c I_c T_{Hc} + 0.5 I_c^2 R_c - k_c (T_{Hc} - T_{Lc}) \tag{2}$$

The input voltage

$$V_c = \alpha_c (T_{Hc} - T_{Lc}) + I_c R_c \tag{3}$$

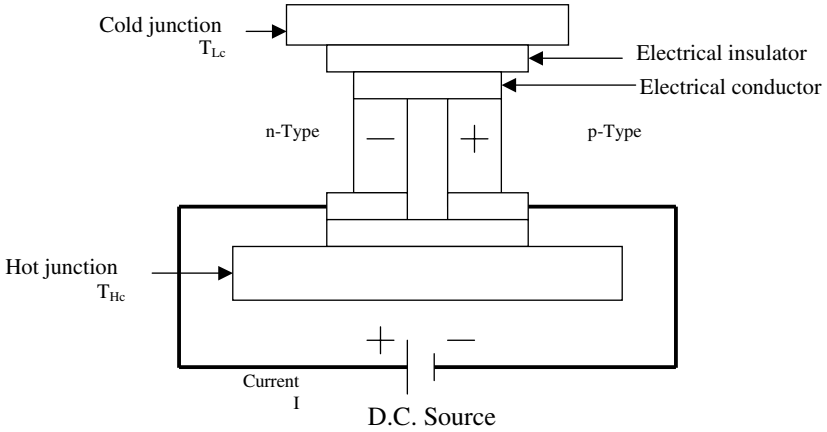


Fig. 1. Schematic diagram of the thermoelectric cooler.

The input power

$$P_c = \alpha_c I_c (T_{Hc} - T_{Lc}) + I_c^2 R_c \tag{4}$$

and the COP

$$\mathrm{COP} = Q_{Lc}/P_c \tag{5}$$

The figure of merit for the TE module, which indicates its quality, is defined as:

$$Z = \alpha^2/kR \tag{6}$$

### 2.2. Thermoelectric generator

The schematic diagram of the TEG is shown in Fig. 2. Like the TEC, it consists of two dissimilar materials, n- and p-semiconductors, connected electrically in series and thermally in parallel. Heat is supplied at one end at temperature $T_{Hg}$, while the other end is maintained at a lower temperature $T_{Lg}$ by a heat sink. As a result of the temperature difference, a current $I_g$ flows through an external load resistance. The power output depends upon the temperature difference, the properties of the semiconductor materials and the external load resistance (or electric current).

For the heat conduction effect, the Joulean heat and the energy supply or removal to overcome the Peltier effects are combined for the whole generator arrangement. The rate of heat supply and heat removal, useful output power and thermal efficiency are given by Angrist [12] as:

The rate of heat supply

$$Q_{Hg} = \alpha_g I_g T_{Hg} - 0.5 I_g^2 R_g + k_g (T_{Hg} - T_{Lg}) \tag{7}$$

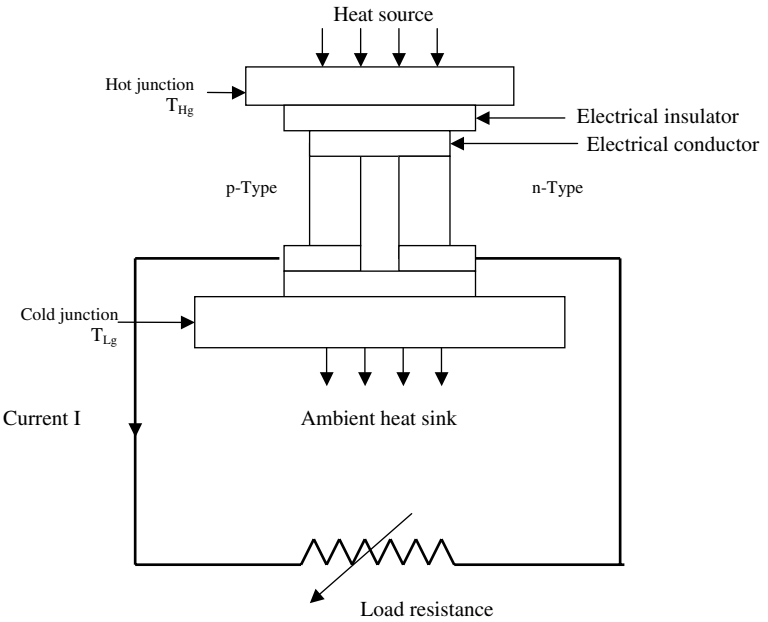


Fig. 2. Schematic diagram of the thermoelectric generator.

The rate of heat removal

$$Q_{Lg} = \alpha_g I_g T_{Lg} + 0.5 I_g^2 R_g + k_g (T_{Hg} - T_{Lg}) \tag{8}$$

The output voltage

$$V_g = \alpha_g (T_{Hg} - T_{Lg}) - I_g R_g \tag{9}$$

The useful output power

$$P_g = \alpha_g I_g (T_{Hg} - T_{Lg}) - I_g^2 R_g \tag{10}$$

and thermal efficiency

$$\eta = P_g / Q_{Hg} \tag{11}$$

### 2.3. TEG–TEC system

In the proposed TEG–TEC system, each module has its own heat sink and the same current passes through the two modules, $I_c = I_g$ and $V_c = V_g$. From Eqs. (3) and (9), we can get;

$$\alpha_c (T_{Hc} - T_{Lc}) + I R_c = \alpha_g (T_{Hg} - T_{Lg}) - I R_g \tag{12}$$

$$I = \alpha_g (T_{Hg} - T_{Lg}) - \alpha_c (T_{Hc} - T_{Lc}) / (R_g + R_c) \tag{13}$$

The feasibility of optimum performance of the system based on the maximum output power of the TEG and maximum cooling capacity of the TEC will be examined to determine the number of generators required to drive the TEC. Eqs. (1) and (10) show that the cooling load of the TEC and the output power of the TEG are functions of the current. Equating the first partial derivative with respect to $I$ to zero in the appropriate equations and solving for an optimum current will maximize these quantities. For the maximum cooling capacity of the TEC, we obtain

$$I_{c(opt)} = (\alpha_c T_{Lc}) / R_c \tag{14}$$

and for the maximum output power from the TEG, we obtain

$$I_{g(opt)} = \alpha_g (T_{Hg} - T_{Lg}) / 2 R_g \tag{15}$$

The optimum performance of the TEG–TEC will be achieved only if the current satisfies both Eqs. (14) and (15) as follows:

$$I_{c(opt)} = n I_{g(opt)} \tag{16}$$

and hence,

$$(\alpha_c T_{Lc}) / R_c = n \alpha_g (T_{Hg} - T_{Lg}) / 2 R_g \tag{17}$$

where $n$ is the number of generators, equal to or more than one. So,

$$n = \frac{2 \alpha_c T_{Lc}}{\alpha_g \Delta T_g} \cdot \frac{R_g}{R_c} \tag{18}$$

Eq. (18) shows that the number of generators is to be selected in accordance with the temperature difference across the generator, the cooling temperature and the properties of the materials of both modules. The maximum power of the generator can be achieved only if the TEC internal resistance is closely matched to the internal resistance of the TEG. This condition is hard to realize since $R_c$ and $R_g$ are not usually equal. Therefore, optimum performance of the system based on both maximum output power of the TEG and maximum cooling capacity of the TEC cannot easily be realized.

An alternative optimum performance of the system may be based on the maximum cooling capacity only. In this case, the number of generators is chosen so as to supply the TEC with its optimum current as determined in Eq. (14). So,

$$I_{c(opt)} = nI_g \tag{19}$$

In actual cases, $I_g$ is not constant as it is a function of the temperature difference $\Delta T_g$ across the generator, which, in turn, is a function of the heat input to the system (solar system). So, the number of generators required to achieve the optimum TEC current in the summer season will not provide the optimum conditions in the winter. On the other hand, the performance of the TEC is better in the winter than in the summer season, while in the rest of the year, the system performance will be between the performances of the two seasons. In determining the number of generators for the TEG–TEC system, the above conditions must be taken into consideration, which requires a detailed study of the system all year round.

## 3. Performance tests of TEC and TEG

The cross-sections of both the TEC and TEG are shown in Figs. 3 and 4, respectively. The TEC, CZ-1.0-127-1.27 Z-MAX, module is made of bismuth telluride based alloys and consists of 127 active couples. It consists of the TEC and two heat exchangers made with aluminum fins. A small fan is used to cool the heat sink exchanger. The cold exchanger is immersed in an insulated water box of 1.35 l volume.

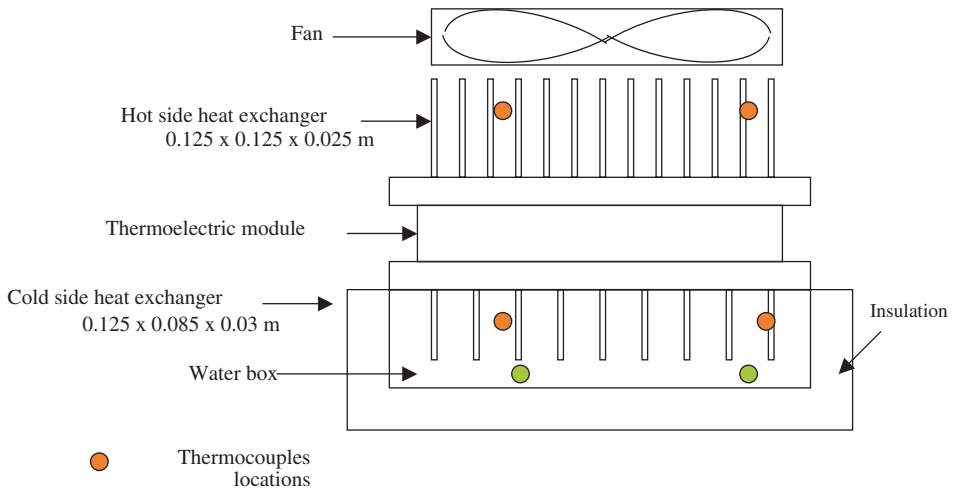


Fig. 3. Cross-section of thermoelectric cooler.

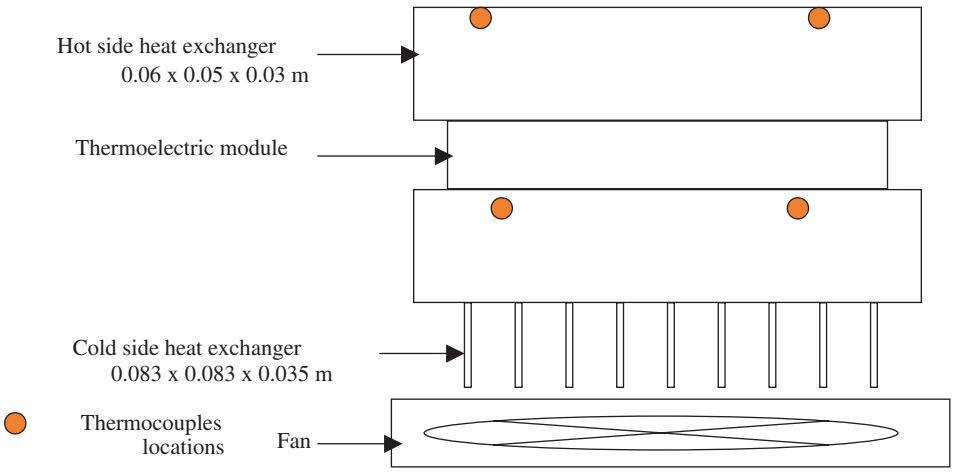


Fig. 4. Cross-section of thermoelectric generator.

The TEG, HZ-14, module is made of bismuth telluride based alloys and consists of 49 active couples. It consists of the TEG, aluminum plate and aluminum heat exchanger with fins. A small fan is used to cool the heat sink exchanger.

### 3.1. Determination of the physical properties of the TEC and TEG

The thermal performance of the TE module depends on the physical properties such as the Seebeck coefficient ($\alpha$), the electric resistance ($R$) and the thermal conductivity ($k$). These properties, which may vary with operating temperature, will be determined from the theoretical equations of the two modules and the experimental results as follows:

1. Measuring the hot end ($T_H$) and the cold end ($T_L$) temperatures. The induced thermoelectric voltage $V$ and the Seebeck coefficient ($\alpha$) can be measured directly from Eqs. (3) and (9) with $I = 0$ for the TEC and TEG, respectively.
2. Measuring the cooling capacity ($Q_L$). The thermal conductivity ($k$) can be determined from Eq. (1) for the TEC with $I = 0$. The cooling capacity of the TEC is measured as the rate of change of the cold water temperature.
3. Measuring the rate of heat input ($Q_H$). The thermal conductivity ($k$) can be determined from Eq. (7) for the TEG with $I = 0$. The rate of heat input of the TEG is measured as the rate of change of the hot plate temperature.
4. Measuring various values of $V$ at various $I$, $T_L$ and $T_H$. With the calculated $\alpha$, the total resistance ($R$) can be determined from Eqs. (3) and (9) for the TEC and TEG, respectively.

### 3.2. Measured parameters and measuring instruments

In the indoor performance tests of the TEC modules, we need to measure the cold side, hot side and water temperatures. Also, in the indoor performance tests of the TEG, we need to measure

the cold side, hot side and heating plate temperatures. We need also to measure the ambient conditions, as well as the currents and voltages in all tests. The cooling capacity of the TEC is calculated as the rate of change of the water temperature in the water box, while the heat input to the TEG is calculated as the rate of change of the heating plate temperature. For outdoor tests, all the previous parameters are measured in addition to the solar intensity and wind speed.

K-type thermocouples are used to measure all temperatures. Two thermocouples are used for each plate. The locations of the thermocouples are shown in Figs. 3 and 4. The thermocouples are connected to a hybrid multi-channel recorder (Model AH520 0NN- NO. AH95A001) to display and record the temperatures of the thermocouples with an accuracy of ±0.1 °C. A data logger weather station (type Delta-T Logger DL 2e) is used to record the ambient conditions, incident solar radiation on a horizontal surface with an accuracy of 5 W/m$^2$ and wind speed with an accuracy of 0.001 m/s. A Digital Multimeter (EXTECH 383273) with PC interface is used to measure the voltage with an accuracy of 0.001 V and the current with an accuracy of 0.01 A.

### 3.3. Error analysis

The uncertainty in the calculated results on the basis of the uncertainties in the primary measurements are given by Kline and McClintock [13] and Dieck [14] as:

$$\omega_s = \left[ \left( \frac{\partial S}{\partial X_1} \right)^2 \omega_1 + \left( \frac{\partial S}{\partial X_2} \right)^2 \omega_2 + \cdots + \left( \frac{\partial S}{\partial X_n} \right)^2 \omega_n \right]^{1/2} \tag{9}$$

where $\omega_s$ is the uncertainty in the result and $\omega_1, \omega_2, \ldots, \omega_n$ are the uncertainties in the independent variables, while $S$ is a given function of the independent variables, $X_1, X_2, \ldots, X_n$. The calculated uncertainties for the different parameters are shown in Table 1.

The obtained physical properties of both modules are shown in Table 2. The results show that $\alpha$, $R$ and $k$ are slight functions of the operating temperatures and, therefore, can be taken as constants during the operation for simplicity.

### 3.4. Performance curves of the TEC

Eqs. (1)–(3) show that the performance of the TEC is a function of the current supply ($I$), hot and cold plates temperatures ($T_{Hc}$ and $T_{Lc}$) and temperature difference across the cooler ($\Delta T_c$).

Table 1
Calculated uncertainties for different parameters

| Parameters | Minimum error (%) | Maximum error (%) |
|---|---|---|
| Temperature | 0.04 | 2 |
| Incident solar radiation | 0.5 | 3.3 |
| Current | 0.166 | 1 |
| Voltage | 0.08 | 0.1 |
| Wind speed | 0.066 | 0.2 |
| Energy rate | 0.44 | 2.1 |
| Seebeck coefficient | 0.89 | 1.44 |
| Thermal conductivity | 0.13 | 0.3 |
| Resistance | 0.97 | 1.04 |

Table 2
Measured physical properties per couple for thermoelectric modules

| Parameter | TEG | TEC |
|---|---|---|
| $\alpha$ (V/K) | $424 \times 10^{-6}$ | $338 \times 10^{-6}$ |
| $R$ ($\Omega$) | 0.0297 | 0.0211 |
| $k$ (W/K) | 0.0045 | 0.005 |
| $Z$ (1/K) | $1.35 \times 10^{-3}$ | $1.08 \times 10^{-3}$ |
| No. of thermocouples | 49 | 127 |

The performance curves of the TEC module are drawn for the various measured cooling capacities, current supplies and heat sink temperatures. The direct currents used in the tests are between 1 and 4 A, and the heat sink temperatures are between 23 and 39 °C.

Figs. 5–7 show the variation of the cooling capacity with the temperature difference $\Delta T_c$ at different $I$ and $T_{Hc}$. It is obvious from these figures that increasing the current supply or reducing $\Delta T_c$ could increase the cooling capacity. These curves help to find the cooling capacity for such operating conditions ($I$, $T_{Hc}$ and $T_{Lc}$) or to determine the operating conditions ($I$, $T_{Hc}$ and $T_{Lc}$) required to satisfy a certain cooling load. The figures also show that to achieve a temperature equal to or below 0°, the current must be more than 2 A, depending on the heat sink temperature.

Using a least square fit to the experimental results yields the following empirical relations:

$$Q_{Lc} = (-0.0038T_{Hc} - 0.6146)\Delta T_c - aI_c^2 + bI_c + c \tag{20}$$

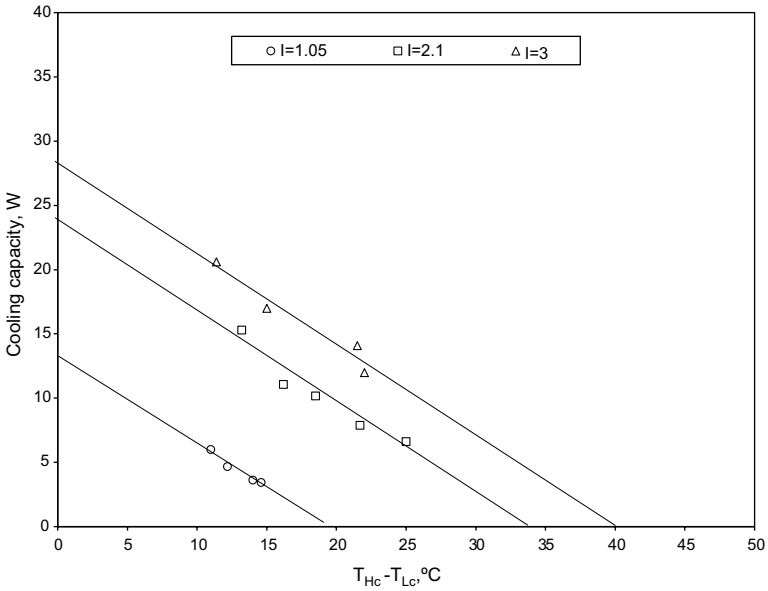


Fig. 5. Variation of cooling capacity with temperature difference across the TEC at different input current ($T_{Hc} = 23$ °C).

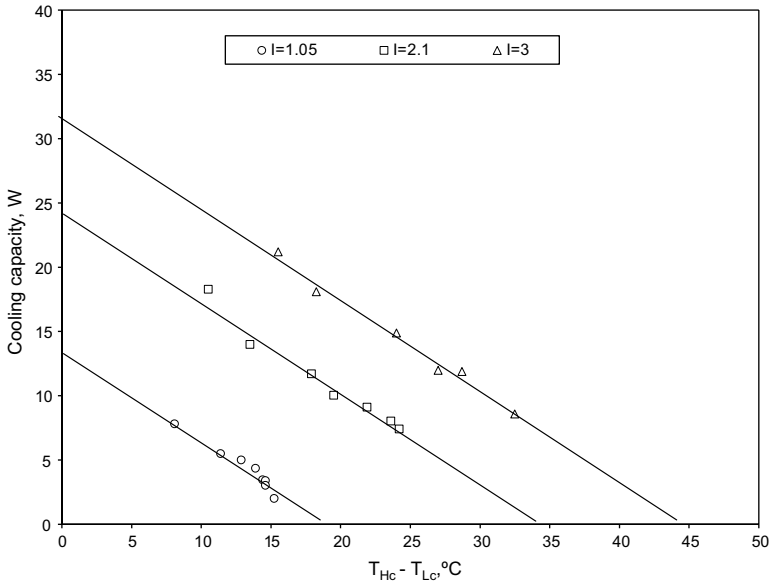


Fig. 6. Variation of cooling capacity with temperature difference across the TEC at different input current ($T_{Hc} = 32$ °C).

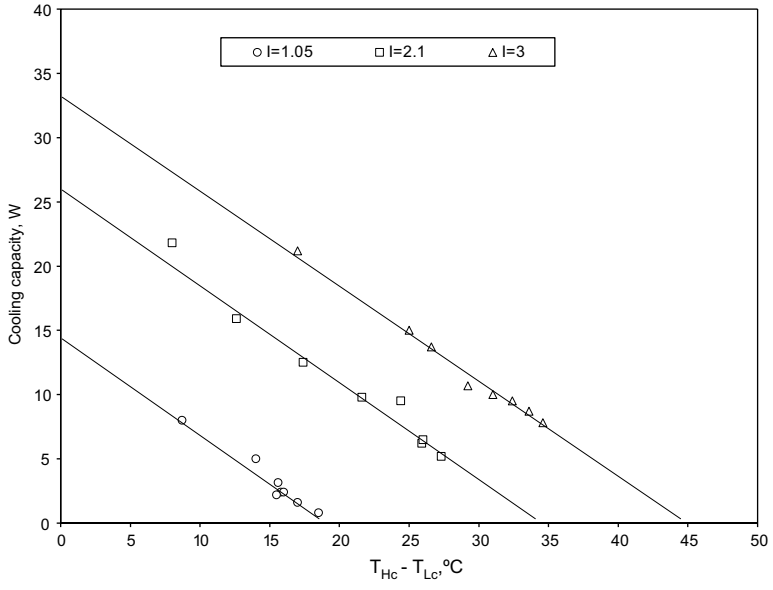


Fig. 7. Variation of cooling capacity with temperature difference across the TEC at different input current ($T_{Hc} = 39$ °C).

where

$$a = 0.0129T_{Hc} + 0.8212 \tag{20-a}$$

$$b = 0.0743T_{Hc} + 12 \tag{20-b}$$

$$c = 0.22T_{Hc} + 0.6128 \tag{20-c}$$

Except for the extreme operating conditions, i.e. at $\Delta T_c$ and $Q_L$ tending to zero or maximum values, the above relations fit the experimental results with an error ranging from 2% to 4%. These relations show that the cooling capacity is a function of the heat sink temperature. The ambient air temperature represents the lower limit of the heat sink temperature, while the upper limit is affected by the operating conditions (fan voltage and input current to the TEC). The effects of these parameters on the rise of the heat sink temperature above ambient ($\Delta T = T_{Hc} - T_{amb}$) are provided in Fig. 8. This figure reveals that $\Delta T$ increases when the fan power decreases or the TEC current increases.

An empirical relation is deduced from the measured values to relate $\Delta T$ with the fan voltage and TEC current as:

For fan voltage = 6 V

$$\Delta T = 2.353\ I - 0.3588, \quad R^2 = 0.96 \tag{21-a}$$

For fan voltage = 3 V

$$\Delta T = 3.828\ I - 0.3013, \quad R^2 = 0.97 \tag{21-b}$$

Eqs. (1)–(5), (20) and (21) are the performance equations for the TEC module. Using these equations and the measured physical properties, we can perform the system analysis of the TEC.

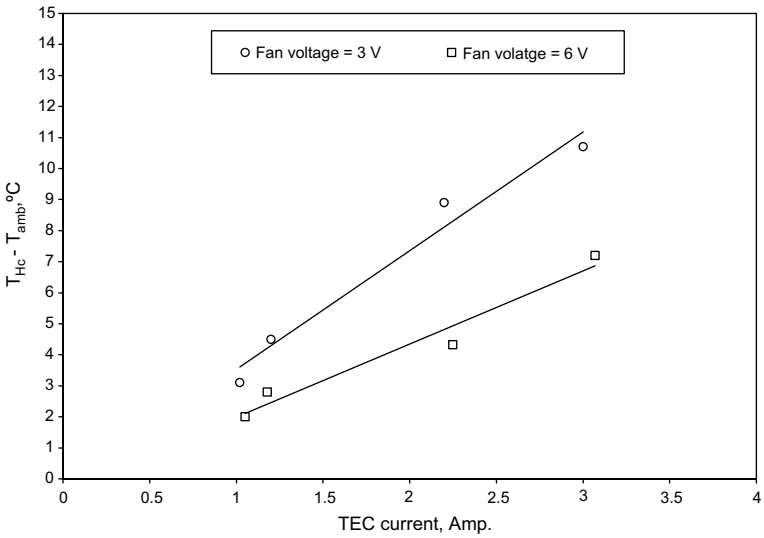


Fig. 8. Variation of temperature difference ($T_{Hc} - T_{amb}$) with TEC current and fan voltage.

### 3.5. Performance curves of TEG

The performance of the TEG is investigated with the TEC connected as an external load. The heating element is insulated. It is assumed that the physical properties $\alpha$, $R$ and $k$ are constants for both modules for simplicity. The measured hot side temperature $T_{Hg}$, the cold side temperature during operation $T_{Lg}$, the temperature difference across the generator $\Delta T_g$ and the output current $I_g$ are drawn for different values of heat input $Q_{Hg}$ in Fig. 9. A least square fit to the test results yields the empirical relations for the generator performance as a function of the heat input:

$$T_{Lg} = 1.0981Q_H + 23.1, \quad R^2 = 0.96 \tag{22-a}$$

$$\Delta T_g = 0.0908Q_H^2 - 0.6816Q_H + 4.0703, \quad R^2 = 0.9971 \tag{22-b}$$

$$T_{Hg} = 0.101Q_H^2 - 0.976Q_H + 23.605, \quad R^2 = 0.9986 \tag{22-c}$$

$$I = 0.0013Q_H^2 - 0.0055Q_H - 0.0916, \quad R^2 = 0.998 \tag{22-d}$$

Fig. 10 shows the variation of the output generator current $I_g$ and the temperature difference across the TEC $\Delta T_c$ with the temperature difference across the generator $\Delta T_g$. The figure shows that for $\Delta T_g$ of 200 °C, the output current does not exceed 1.03 A. This result is expected since the number of couples of the cooler is more than double that of the generator. The current calculated from Eq. (13) will be small. Added to this, the differences in the physical properties of both modules is slight. So, more than one generator must be used to achieve a higher current supply for the TEC.

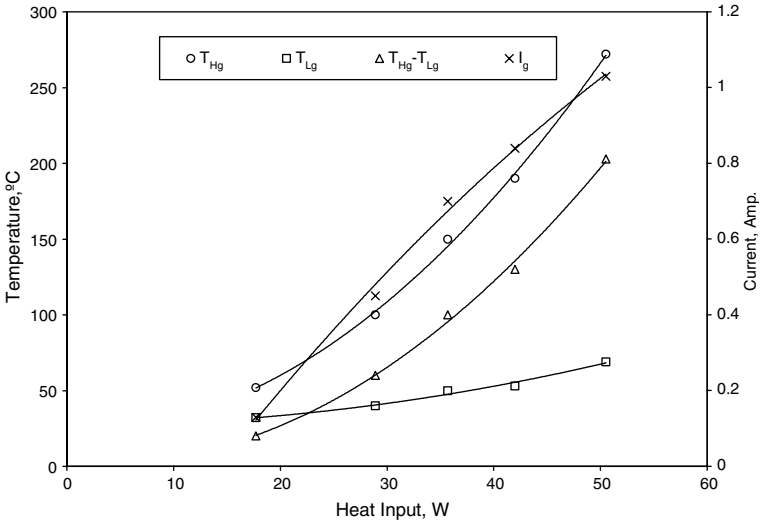


Fig. 9. Variation of hot side temperature $T_{Hg}$, cold side temperature $T_{Lg}$, temperature difference $T_{Hg} - T_{Lg}$ and produced current $I$, with heat input to the generator $Q_{Hg}$.

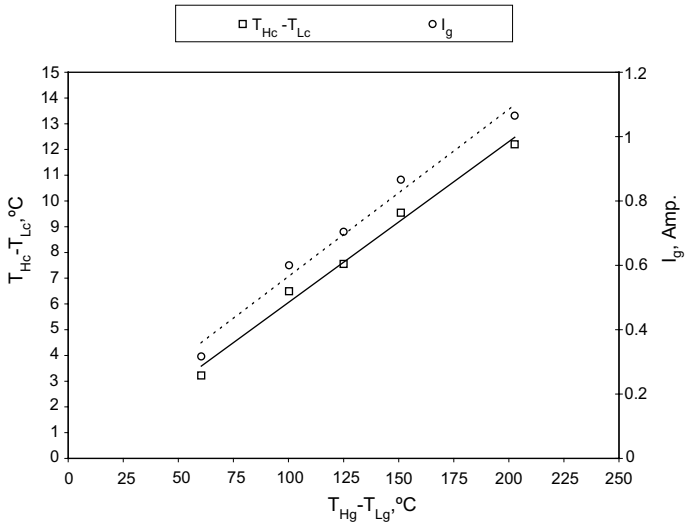


Fig. 10. Variation of the generator current, $I_g$, and temperature difference, $T_{Hc} - T_{Lc}$, across the cooler with the temperature difference, $T_{Hg} - T_{Lg}$, across the generator.

## 4. Simulation of the solar TEG–TEC system

Fig. 11 shows an overview of the solar box with the solar reflectors that heat the TEG in the TEG–TEC system. A black absorber made of aluminum plate ($0.3 \times 0.3 \times 0.2$ m) is joined to the hot plate of the TEG. The system is placed in a wood insulated box. The upper surface of the heating plate is covered with two layers of 3 mm glass window. A simple arrangement of plane

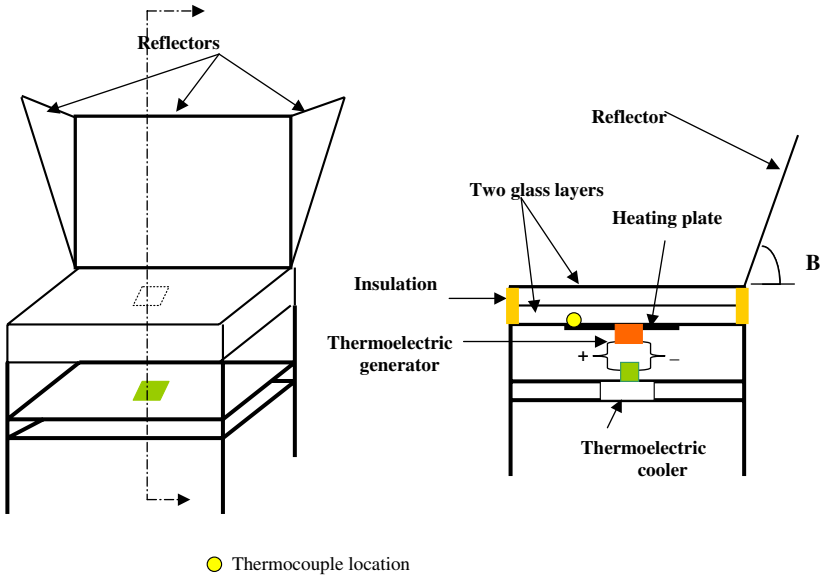


Fig. 11. The solar reflector arrangement used to heat the TEG.

Table 3
Inclination angles, $\beta$, and concentration factors, CF, for different reflector arrangements

| Months | Type A | |
|---|---|---|
| | $\beta$ (°) | CF |
| January | 94 | 1.9 |
| February | 89 | 1.87 |
| March | 80 | 1.63 |
| April | 73 | 1.45 |
| May | 68 | 1.35 |
| June | 66 | 1.25 |
| July | 68 | 1.3 |
| August | 74 | 1.4 |
| September | 80 | 1.5 |
| October | 92 | 1.75 |
| November | 89 | 2.0 |
| December | 96 | 1.91 |

reflectors is used to heat the absorber. The inclination angles of the reflector arrangements are chosen according the analysis of Ref. [15] to receive the maximum energy input at noon time throughout the year. Table 3 shows the angles of inclination and concentration factors for all year round. The rear side of the plate is insulated with foam ($k = 0.045$ W/mK).

### 4.1. Simulation of the TEG performance

The model simulating the TEG performance is based on Eqs. (6)–(10), the measured physical properties, the empirical relations (22a–d) and the following heat balance equation for the heating plate under steady state conditions:

$$A(\mathrm{SI}(\tau\alpha) - U_{\mathrm{T}}(T_{\mathrm{P}} - T_{\mathrm{amb}})) = Q_{\mathrm{Hg}} \tag{23}$$

So,

$$T_{\mathrm{P}} = ((A\mathrm{SI}(\tau\alpha) - Q_{\mathrm{Hg}})/AU_{\mathrm{T}}) - T_{\mathrm{amb}} \tag{24}$$

where $A$ is the heating plate area and $U_{\mathrm{T}}$ is the top loss coefficient, calculated according to Duffie and Beckman [16] as:

$$U_{\mathrm{T}} = \left\{ \frac{N}{C/T_{\mathrm{P}}\left[\frac{T_{\mathrm{P}}-T_{\mathrm{amb}}}{(N+f)}\right]^{e}} + \frac{1}{h_{\mathrm{w}}} \right\}^{-1} + \frac{\sigma(T_{\mathrm{P}} + T_{\mathrm{amb}})(T_{\mathrm{P}}^2 + T_{\mathrm{amb}}^2)}{(\varepsilon_{\mathrm{P}} + 0.00591Nh_{\mathrm{w}}) + \frac{2N+f-1+0.133\varepsilon_{\mathrm{P}}}{\varepsilon_{\mathrm{g}}} - N}$$

where

$$f = (1 + 0.089h_{\mathrm{w}} - 0.1166h_{\mathrm{w}}\varepsilon_{\mathrm{g}})$$
$$e = 0.43(1 - 100/T_{\mathrm{g}})$$
$$C = 520(1 - 0.000051\beta^2)$$

and the wind heat transfer coefficient is

$$h_{\mathrm{w}} = 4.9 + 3.8V$$

The other parameters are $N = 2$, $\varepsilon_g = 0.8$, $\varepsilon_P = 0.8$ and $\beta = 0$.

The meteorological data all year round for the Cairo location (30°N latitude) is used in the simulation

The above model is solved by iteration methods as follows:

1. Choose $T_P$ then from Eq. (23) calculate $Q_{Hg}$.
2. The obtained $Q_{Hg}$ is used to determine $\Delta T_g$ and $I$ from Eqs. (22b and d).
3. Calculate a new value of $Q_{Hg}$ from Eq. (6) using the obtained parameters in step 2 and the physical properties of the TEG.
4. Compare the new value of $Q_{Hg}$ with that obtained from step 1. If the difference is more than 1%, use the new value of $Q_{Hg}$ obtained in step 3 again in step 2 and repeat until the required accuracy is obtained, then calculate the correct value of $T_P$ from Eq. (24).

To verify the above analysis for the TEG, the system parameters are measured through experimental tests under the actual conditions of Cairo (30°N latitude) during noon time of December. The calculated and the measured temperature of the heating plate temperature $T_P$ and hot side temperature $T_{Hg}$, during noon time are shown in Fig. 12. Comparison between the predicted and measured results show that the model is sufficiently good to simulate the system performance. It is observed from the figure that there is a large difference in the measured temperatures between the heating plate and the generator hot plate. This may be attributed to the following reasons:

1. The energy transferred by conduction through the module legs.
2. Part of the generator energy is lost as it is exposed to ambient at the fan connection. These losses increase as the ambient temperature decreases.
3. The contact between the two plates is not good although thermal paste is used.

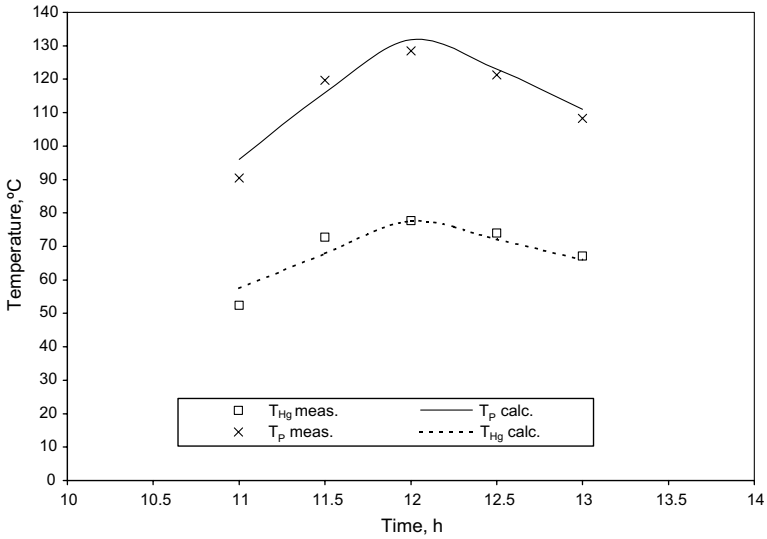


Fig. 12. Calculated and measured heating plate and generator hot plate temperatures.

### 4.2. Prediction of the TEG–TEC system performance

Eqs. (6)–(10), the empirical relations (22) and (23) are used to predict the TEG performance all year round under the actual conditions of the Cairo climate (30°N latitude). Fig. 13 shows both the average total solar intensity incident on a horizontal surface during the noon hours (with and without concentration) and the concentration factor (CF) for different months of the year. Fig. 14 shows the predicted values of $T_P$, $T_{Hg}$, $\Delta T_g$ and the output current all year round. Using a reflector arrangement suited for heating in winter, the CF reaches its highest values during the winter months. This will help to make the energy received by the generator all year round have the same order of magnitude. Fig. 14 shows the flatness of the TEG performance curves that result in nearly constant values of the output current for most months of the year. The maximum difference between the output current during the hottest and coldest months is about 20%, which will ease the choice of the $I_g$ at which $n$ is determined.

The optimum TEC current is calculated from Eq. (18) and found to be between 4.5 and 4.6 A for $T_L = 0$ and 2 °C. The cooling capacity is calculated from Eqs. (21) and (22) at $T_L = 0$ and 2 °C for January and June and shown in Fig. 15. It is found that the optimum cooling capacity is achieved at a current between 4.7 and 4.8 A for $T_L = 0$, and 2 °C, and it has the same value in both months. According to the calculated optimum current, 10–12 TEGs are required to achieve the optimum TEC current for the hot and cold months, respectively.

In order to determine $n$ for best performance all year round, the cooling capacity achieved every month of the year when using 9, 10, 11 and 12 generators are calculated for $T_{Lc} = 0$ and 2 °C, respectively. Figs. 16a and b show these values. From the obtained results, it is evident that as

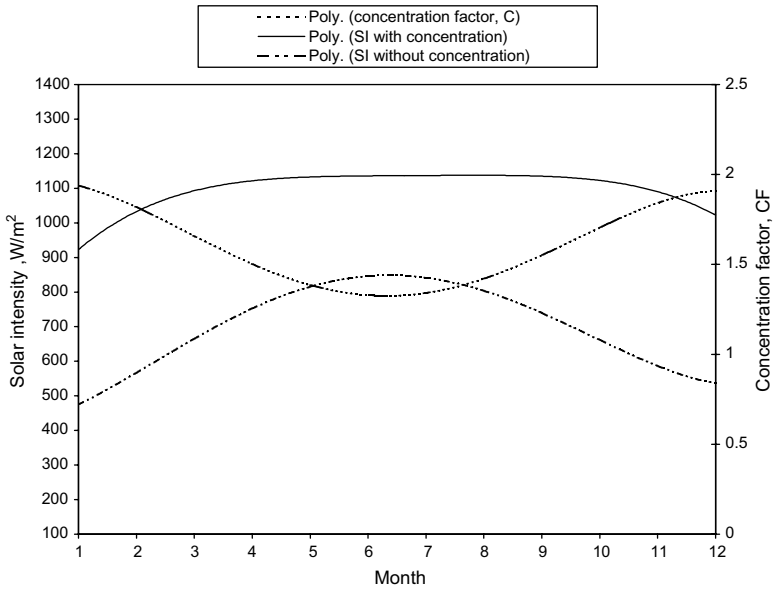


Fig. 13. Average total solar intensity on horizontal surface and concentration factor at noon time all year round.

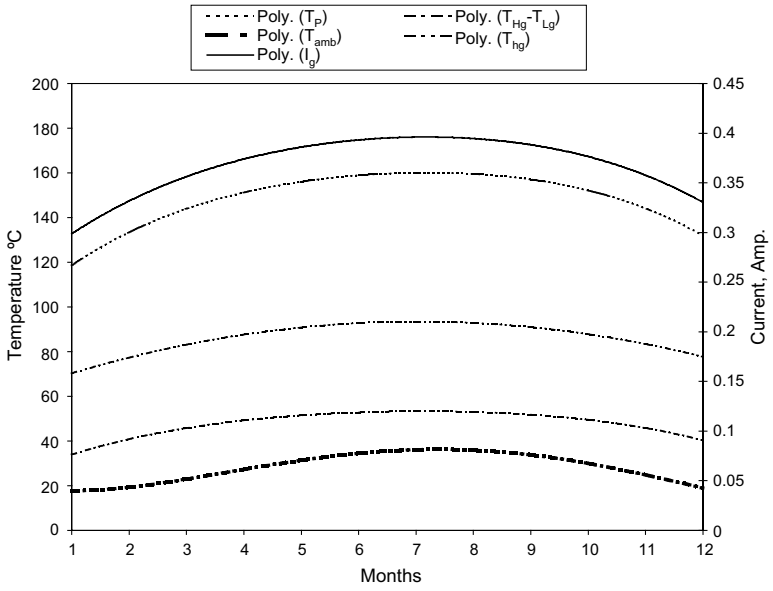


Fig. 14. Predicted performance of the thermoelectric generator all year round.

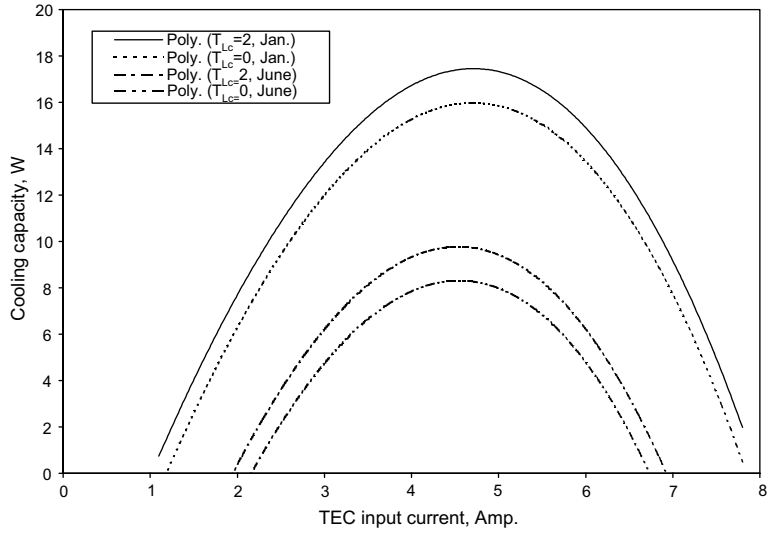


Fig. 15. Variation of cooling capacity with TEC current at January and June for cold side temperature $T_{Lc} = 0$ and 2 °C.

the number of generators increases, the output current increases and approaches the value of the optimum TEC current. The cooling capacity increases with the increase of the input current until it reaches the optimum value and then decreases again. This number is 10 TEGs for summer and 12 TEGs for winter. So, $n = 11$ TEGs can give adequate cooling capacity for more than 8 months of the year. From this value, we find that the required ratio for the TEG couples to the TEC couples is $11 \times 49/127 = 4.25$.

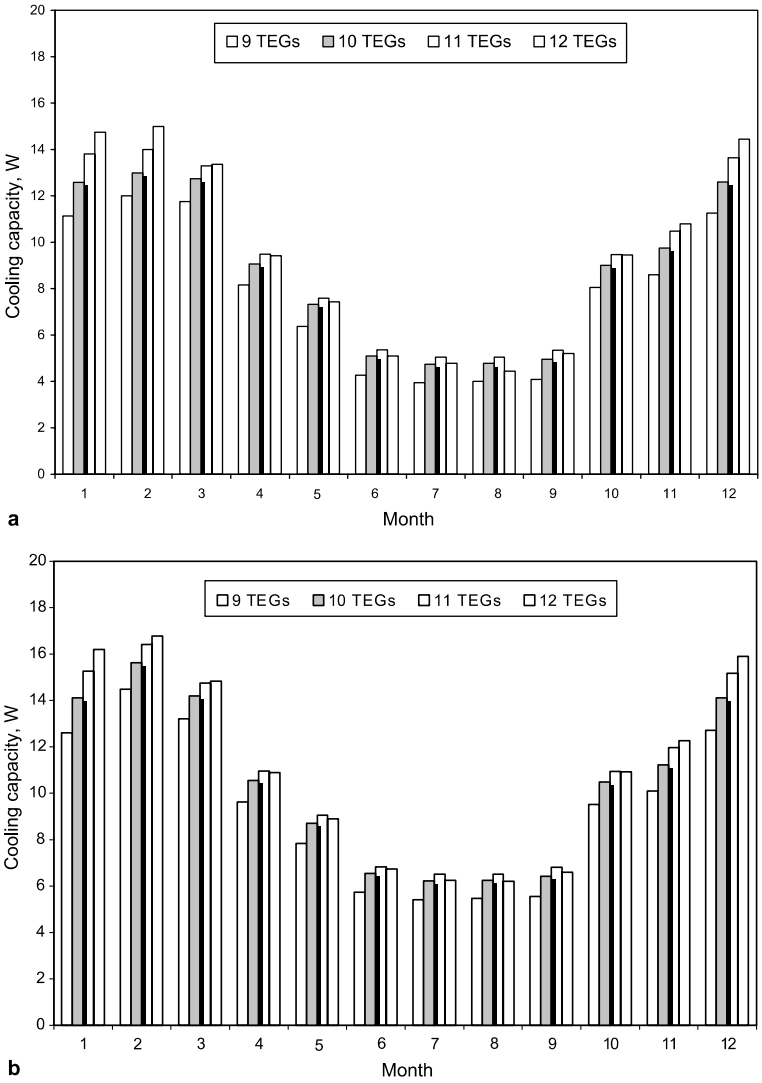


Fig. 16. (a) Variation of cooling capacity of the TEC with number of TEGs, $T_L = 0\,^{\circ}C$. (b) Variation of cooling capacity of the TEC with number of TEGs, $T_L = 2\,^{\circ}C$.

## 5. Conclusions

The possibility of using a solar thermoelectric generator to drive a small thermoelectric cooler is studied. The number of TEG modules required to power the TEC that achieve the best performance of the TEG–TEC system all year round is determined from the performance test results of both modules and the mathematical model simulating the system performance. A simple arrangement of plane reflectors is proposed to heat the TEG. This arrangement has the advantage of its suitability for efficient heating in winter.

It is found from this study that five thermocouples of the TEG can drive one thermocouple of the TEC. This means that the used TEG modules are required to power the used TEC at optimum performance most times of the year.

## References

[1] Threlkeld JL. Thermal environmental engineering. Prentice-Hall; 1962 [Chapter 6].
[2] Sofrata H. Solar thermoelectric cooling system. In: Proceedings of the Fifth SOLARAS Workshop, Riyad, Saudi Arabia. 1984. p. 59–76.
[3] Dai Y, Wang J, Ni L. Experimental investigation and analysis on a thermoelectric refrigerator driven by solar cells. J Solar Energy Mater Solar Cells 2003;77(4):377–91.
[4] Wu C. Analysis of waste-heat thermoelectric power generators. Appl Thermal Eng 1996;16(1):63–9.
[5] Nuwayhid RY, Rowe DM, Min G. Low cost stove-top thermoelectric generator for regions with unreliable electricity supply. J Renew Energy 2002;28(2):205–22.
[6] Rowe DM. Thermoelectric, an environmentally friendly source of electrical power. J Renew Energy 1999; 16(1–4):1251–6.
[7] Ioffe AF. Semiconductor thermoelement and thermoelectric cooling. London: Info. Search; 1957.
[8] Huang BJ, Chin CJ, Duang CL. A design method of thermoelectric cooler. Int J Refrig 2000;23(3):208–18.
[9] Astrain D, Vian JG, Dominguaz M. Increase of COP in the thermoelectric refrigeration by the optimization of heat dissipation. J Appl Thermal Eng 2003;23(17):2183–200.
[10] Helmers L, Muller E, Schilz J, Kaysser WA. Graded and stacked thermoelectric generators—Numerical description and maximization of output power. J Mater Sci Eng B 1998;56(1):60–8.
[11] Vella GJ, Harris LB, Goldsmid HJ. A solar thermoelectric refrigerator. J Solar Energy 1976;18:355–9.
[12] Angrist SW. Direct energy conversion. 4th ed.. Boston: Allyn and Bacon; 1982.
[13] Kline SJ, McClintock FA. Describing uncertainties in single sample experiments. Mech Eng 1953:3–9.
[14] Dieck RH. Measurement uncertainty method and applications. Research Triangular Park, North Carolina: The Instrument Society of America; 1992.
[15] Helwa NH, El-Swify ME. Performance of portable family size solar box cooker. J Inst Eng (India) 1993;74(September):1–4.
[16] Duffie JA, Beckman WA. Solar engineering of thermal processes. Wiley Interscience; 1991.